Met. Mater. Int., Vol. 21, No. 1 (2015), pp. 1~6
doi: 10.1007/s12540-015-1001-0

Kinetics of Fe_2Al_5 Phase Formation on 4130 Steel by Al Pack Cementation and Its Oxidation Resistance

Y. I. Son[1], C. H. Chung[2], R. R. Gowkanapalli[2], C. H. Moon[3], and J. S. Park[2,*]

[1]Agency for Defense Development, Yuseong, P.O. Box 35-5, Daejeon 305-600, Korea
[2]Hanbat National University, Department of Materials Science & Engineering, Daejeon 305-719, Korea
[3]Hoseo University, School of Display Engineering, Asan 336-795, Korea

(received date: 1 May 2014 / accepted date: 3 June 2014)

Aluminide coatings were developed on low alloy AISI 4130 steel in the temperature range of 500~700 °C by pack cementation method. A Fe_2Al_5 phase was produced on the surface of the steel samples. The coating layer showed a single and a uniform structure. The growth kinetics of the coating layer exhibited a diffusional growth. The activation energy for formation of Fe_2Al_5 was estimated to be 53.7 kJ mol^{-1}. Oxidation tests were carried out for both the aluminized and the bare steels in the temperature range of 500~700 °C. In the case of the coated specimens, the upper region of the aluminide layer was converted to an Al_2O_3 layer. The oxidation resistance tests showed that the presence of Fe_2Al_5 layer increased the oxidation resistance of AISI 4130 steels via formation of the Al_2O_3 layer. The coated specimen exhibited an increased oxidation resistance by about two orders. The kinetics of the coating layer has also been discussed in terms of microstructural observations and estimation of the corresponding parameters.

Keywords: alloys, coating, oxidation, SEM, pack cementation

1. INTRODUCTION

Chrome-moly steel has been widely used for a variety of applications, such as aerospace structural components, welded tubing applications, rock-crushing machinery and automotive parts [1-4]. However, the instability of this type of steel, under high temperature operating conditions imposes serious limitations in their structural applications under severe environments. One of the most plausible explanations for such failure is development of a hematite (Fe_2O_3) layer on top of Cr_2O_3 scales at high temperature (~1000 °C). There arises a mismatch between the thermo-mechanical properties of the two layers, which causes spalling and cracking, and eventually resulting in a significant degradation of their original properties [5,6]. One approach to overcome this problem is through the application of protective coatings on alloy steels. High temperature-resistant coatings are expected to protect the substrate under extreme operating conditions. Among the various deposition techniques, viz. plasma spray, pack cementation, and physical vapor deposition [7-9], the pack cementation process is one of the most effective and inexpensive methods. Thus, pack-aluminizing has been widely used to deposit uniform coating layers on steels [9,10] and superalloys [8,11] in order to improve their high temperature oxidation and corrosion resistance [11,12] properties. Particularly, the formation of iron-aluminides (FeAl, Fe_3Al and Fe_2Al_5) offers a combination of attractive properties, such as low cost, low density, good wear resistance, ease of fabrication and resistance to oxidation and sulphidation at high temperatures [12]. The high temperature resistance of most of these aluminides is based on the formation of a continuous protective layer of Al_2O_3 when exposed to oxidizing atmospheres. Indeed, the coating layer can provide a good diffusion barrier to withstand high temperature oxidation and therefore, increase the life time of steel in aggressive atmospheres [7,12,13].

The present study is aimed to investigate the oxidation resistance of AISI 4130. Diffusion coating layers were developed at relatively low temperatures via pack cementation process and the oxidation resistance of the aluminized and bare steels were evaluated at the temperature range 500-700 °C. Investigated were also conducted on the growth kinetics of iron-aluminide layers, formed by Al pack cementation on AISI 4130 steel substrates, along with studies on the oxidation kinetics of aluminized and bare AISI 4130 specimens.

2. EXPERIMENTAL PROCEDURE

Commercial AISI 4130 steel was used as a starting substrate. Its chemical composition is shown in Table 1. The

*Corresponding author: jsphb@hanbat.ac.kr

Table 1. Chemical composition (wt.%) of AISI 4130 steel

C	Cr	Mn	'Mo	P	Si	S	Fe
0.28	1.1	0.55	0.25	0.035	0.25	0.04	Balance

specimens with dimensions of 10×10×5 mm were polished with a SiC abrasive paper of grade 2000 for finishing, and they were subsequently cleaned using ethanol in an ultrasonicator. The pack cementation process was employed to form a coating layer on the surface of the 4130 steel using a mixture of powder of composition, Al_2O_3 65%, Al 30%, and $AlCl_3$ 5%. Al acted as a depositing source, $AlCl_3$ as an activator and Al_2O_3 as inert filler. A cylindrical alumina crucible (30 mm diameter and 40 mm height) was filled with the above powder mixture. The crucible was vibrated during the various filling stages to obtain a relatively uniform and dense pack.

Only one specimen was placed in the pack, the crucible was then covered with an alumina lid and sealed with alumina cement. The whole pack was loaded into a tube furnace with a continuous flow of Ar gas. The furnace was heated to a desired temperature at a rate of 5 °C/min from room temperature, and was held for desired annealing duration. Selected annealing temperatures were 500, 600 and 700 °C. Heating duration at each desired temperature was varied to 6, 12, and 24 hours. The sample was then cooled to room temperature under Argon. On cooling, the specimen was removed from the crucible and ultrasonically cleaned in ethanol to remove any loosely embedded pack particles.

For static oxidation experiments, both the aluminized AISI steels and bare AISI steels were used. The samples were oxidized at various temperatures of 500, 600, and 700 °C. The oxidation time was also varied, i.e. 30, 50 and 100 hours at each selected temperature. Weight measurements, X-ray diffraction (D/Max 2500H, Rigaku®), scanning electron microscopy (SEM, JEOL-6300), and energy dispersive spectroscopy (EDS) techniques were employed to examine the effect of oxidation on the physical, microstructural, and chemical compositional properties of the samples.

3. RESULTS AND DISCUSSIONS

3.1. Al pack cementation: microstructure and kinetics

The Fe-Al equilibrium phase diagram is shown in Fig. 1. The system is characterized as an iron-based solid solution and six intermetallic compounds of Fe_3Al, FeAl (α2), $FeAl_2$, Fe_2Al_3 (ε), Fe_2Al_5 and $FeAl_3$ (Fig. 12) [14]. In the present study, the Fe-Al intermetallic phase formation during Al pack cementation process was focused. The results of X-ray diffraction of the aluminized coatings at 500 °C for 6, 12 and 24 hours are shown in Fig. 2. All the major peaks of the aluminized surface layer matched well with those of the Fe_2Al_5 phase. The EDS data showed that the concentrations of Fe and Al was 71.61% and 28.39% (Fig. 3), which was

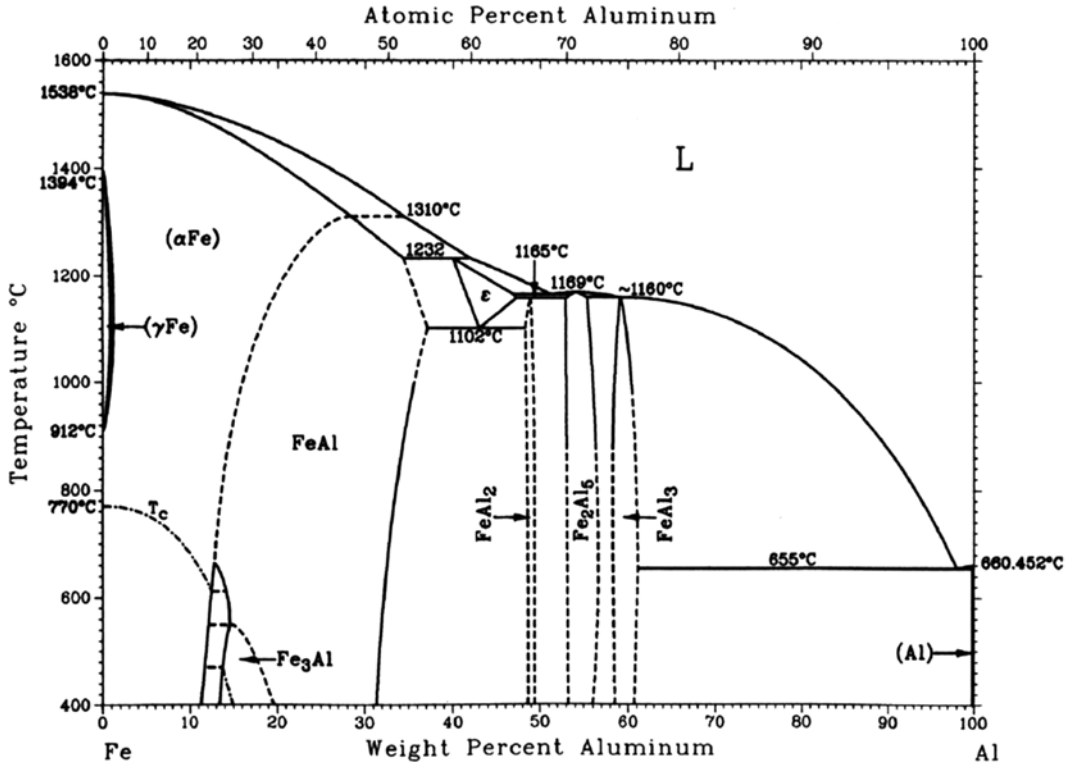

Fig. 1. Fe-Al Phase diagram [14].

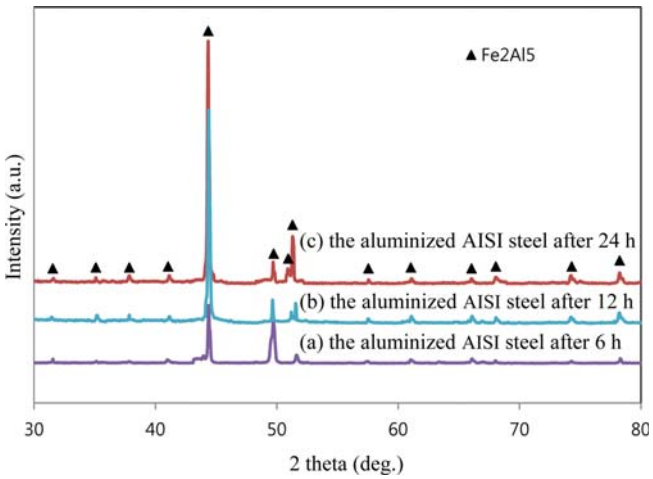

Fig. 2. XRD patterns of aluminized AISI 4130 steel heated at 500 °C for, (a) 6 h, (b) 12 h, and (c) 24 h.

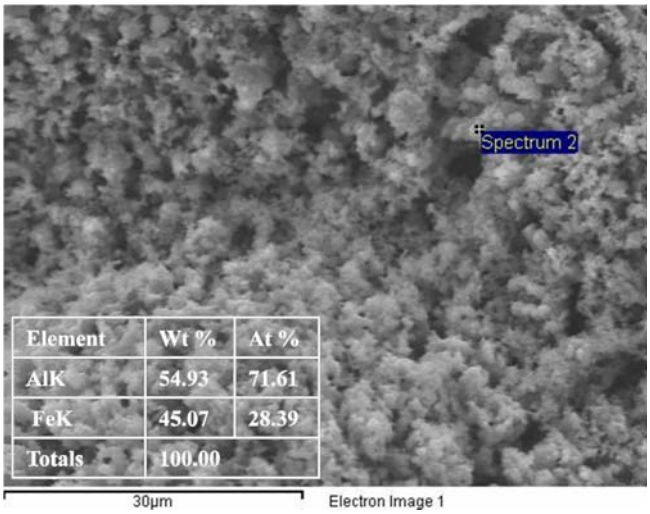

Fig. 3. Surface morphology of the aluminized AISI 4130 steel at 500 ° C for 24 h.

very close to the value of Fe_2Al_5. The XRD and EDS results suggested a Fe_2Al_5 layer was formed on the surface by Al pack cementation process. To further confirm our conclusion, we investigated the cross sectional image of the aluminized layer and its chemical composition (Fig. 4). The EDS results also showed that the Al and Fe concentration across the coating depth remained almost constant with Al to Fe atomic ratio of 2.43. It is thus clear that a uniform single surface layer of Fe_2Al_5 has been formed. Furthermore, these results are congruent with the recent studies of other groups summarized in Table 2. Xiang and Datta [9] and Behrani [15] used similar pack cementation at different temperatures, and Jindal *et al*. [16] used solid state diffusion couple in the formation of Fe-Al intermetallic compounds. In every case the Fe_2Al_5 phase was found to be formed on the surface.

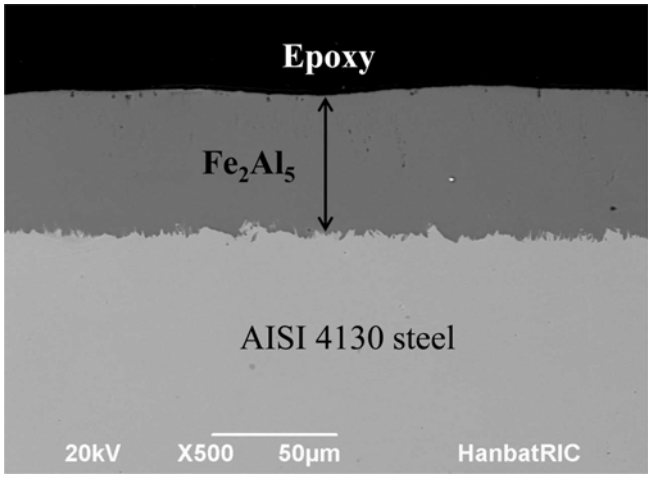

Fig. 4. BSE cross sectional image of the aluminized AISI 4130 steel at 500 °C for 24 hr.

The formation of the intermetallic layer on the steel surface can be represented by the following equation.

$$5\ Al_{diff+}\ 2\ Fe_{diff} = Fe_2Al_5 \quad (1)$$

Diffusion controlled growth kinetics can be written as: $X=k\ t^{0.5}$ where X=coating layer thickness, k=kinetic parameter and t=time. Figure 5 plots the coating layer thickness with respect to the square root of time ($t^{1/2}$), and shows that

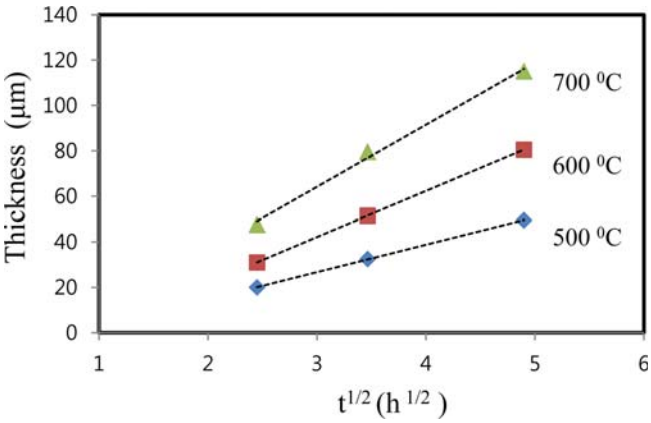

Fig. 5. Plots of Fe_2Al_5 layer thickness as a function of square root of the aluminizing time at 500, 600, and 700 °C, showing the growth kinetics of Fe_2Al_5 layer on AISI 4130 steel.

Table 2. Results from recent literature of the Fe-Al system

Reference	Processing Method	Annealing Temperature	Intermetallics Detected	Activation Energy (Q) kJ mol^{-1}
[9]	Pack cementation	650 °C	Fe_2Al_5	73.33
[15]	Pack cementation	650-900 °C	Fe_2Al_5	68.58
[16]	Solid state diffusion couple	500 °C	Fe_2Al_5	-

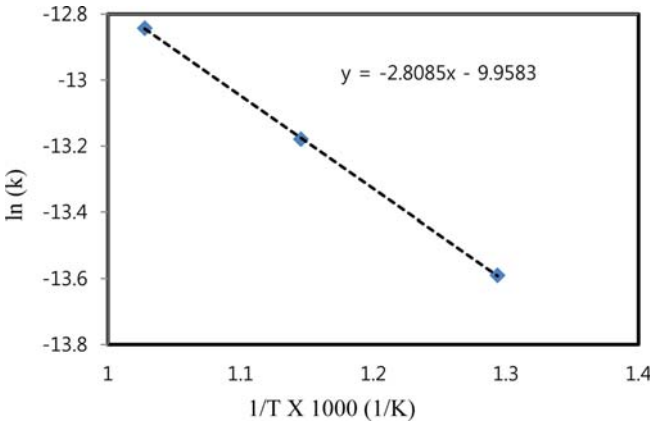

Fig. 6. Plot of kinetic parameter (k) versus the aluminizing temperature T for the Fe_2Al_5 layer.

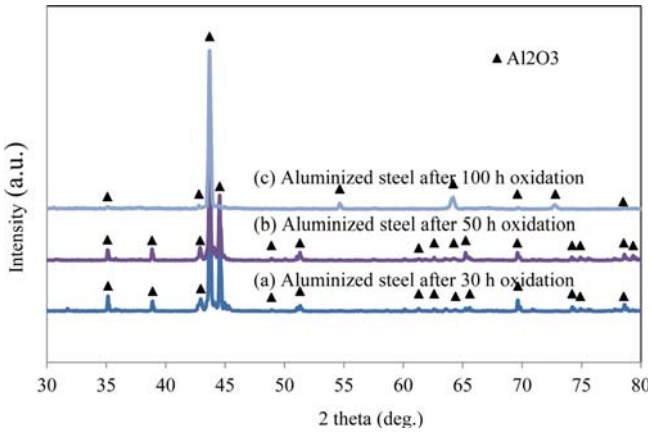

Fig. 7. XRD patterns of AISI 4130 steel, which was sequentially aluminized and oxidized at 500 °C for, (a) 30 h, (b) 50 h, and (c) 100 h.

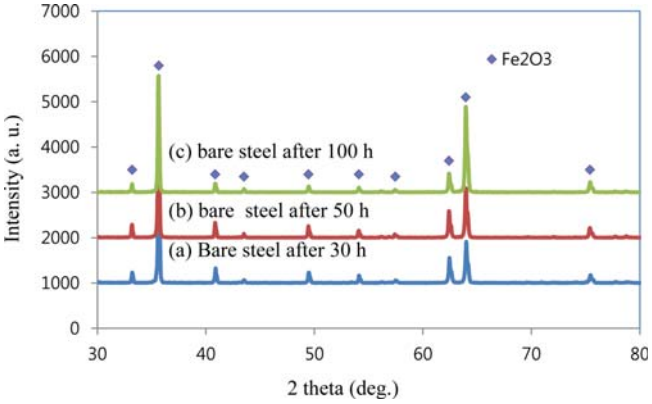

Fig. 8. XRD patterns of bare AISI 4130 steel oxidized at 500 °C for, (a) 30 h, (b) 50 h, and (c) 100 h.

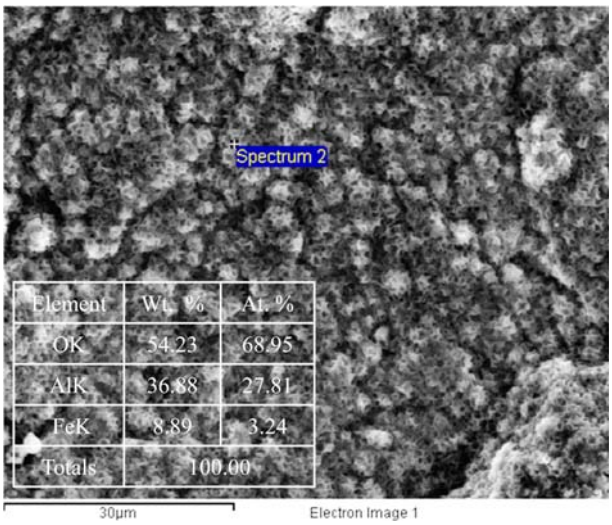

Fig. 9. Surface morphology of aluminized AISI 4130 steel after oxidation at 500 °C for 30 h.

the growth kinetics of the coating layer follows a diffusional mode. The kinetic parameter values were estimated to be 9.62, 15.44 and 22.74 for the growth temperature of 500, 600 and 700 °C, respectively. A higher value of the kinetic parameter with increasing temperature indicates that a higher deposition rate can be obtained at a higher growth temperature.

Figure 6 plots natural log of the kinetic parameter as a function of 1/T (T is the absolute temperature). It essentially shows a linear relationship, suggesting that a simple Arrhenius relationship can be used to describe the effect of temperature on the growth rate (k):

$$\ln k = - Q/ (RT) + C \quad (2)$$

where, Q is the activation energy, R the gas constant and C is a constant. A least square fit to the data gave a slope 2.81 for the straight line, from which the activation energy calculated was 53.70 kJ mol^{-1}. The activation energy values reported by other researcher are summarized in Table 2. Vikas Behrani [15] calculated the activation energy as 68.58 kJ mol^{-1} for Al pack cementation processing in the range 650-900 °C on commercial carbon steel tube SA210 (Fe-0.93Mn-0.27C-0.1Si) [15]. Xiang and Datta estimated the activation energy to be 73.33 kJ mol^{-1} and 77.3 kJ mol^{-1} for p-92 alloy steel (Fe-2.25Cr-1.0C) and for low alloy steel (Fe-9Cr-1.0Mo-0.1C), respectively [9,17]. The above reported values are slightly are higher than the activation energy obtained in the current study. This is probably because the kinetics of formation of aluminide coatings on steel depends on the structure of the substrate steel, the alloying elements, the structure of the coating formed, and the coating process parameters.

3.2. Oxidation resistance: microstructure and kinetics

The static oxidation treatment of aluminized AISI 4130 steel resulted in the formation of an Al_2O_3 layer on the top of the Fe_2Al_5 layer. EDS (Fig. 9) and XRD (Fig. 7) data confirmed the formation of the Al_2O_3 layer on the surface. A minor amount of Fe (3.24%) was also detected in the EDS analysis, which was due to some left over Fe_2Al_5 layer. EDS

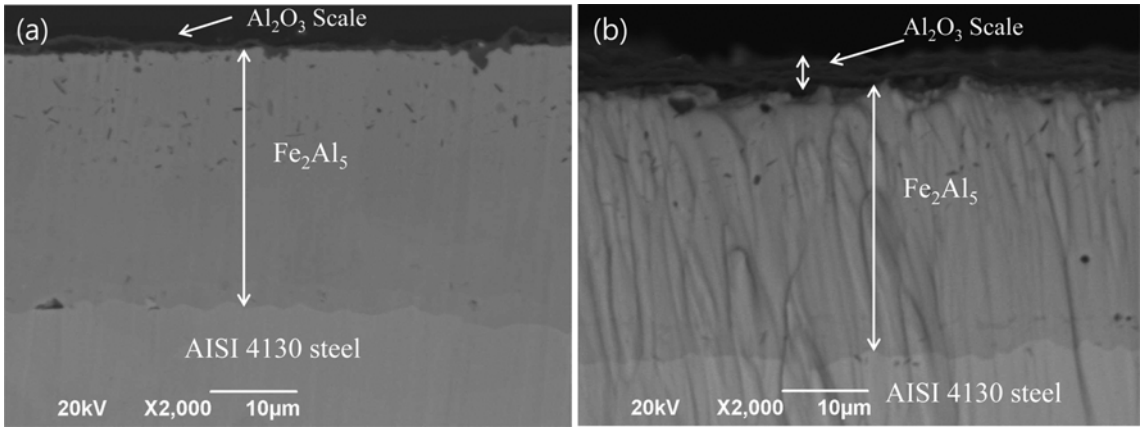

Fig. 10. BSE cross sectional images of AISI 4130 steel, which was sequentially aluminized and oxidized, (a) at 500 °C for 30 h, and (b) at 700 °C for 100 h.

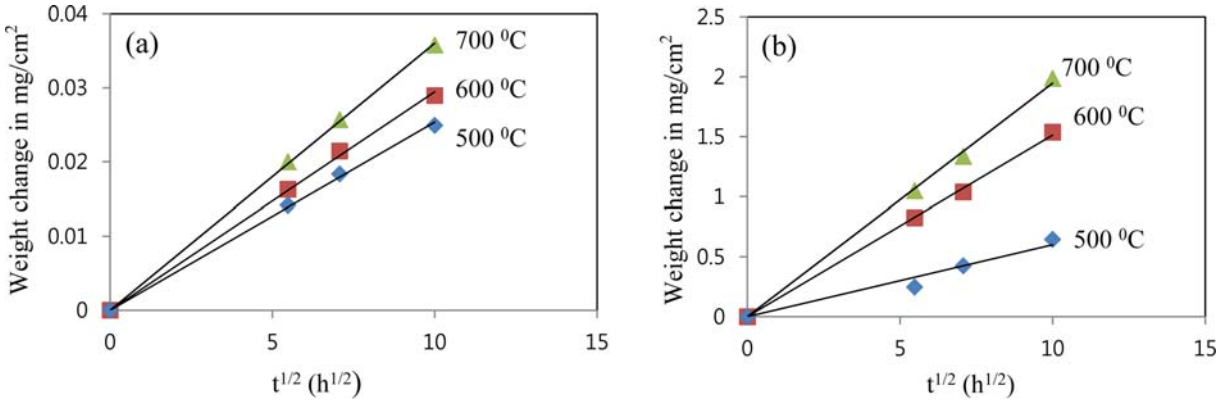

Fig. 11. Weight change *vs* time^{½} of (a) the aluminized AISI 4130 steel and (b) bare AISI 4130 steel, oxidized at 500, 600, and 700 °C in air.

analysis of the cross section further confirmed the formation of a continuous Al_2O_3 scale on the top of the steel surface (Fig. 10). The cross section image shows a good bonding between the coating layer and the oxide layer on the steel surface. The thickness of Al_2O_3 layer was 2 μm and 4 μm under the oxidation conditions of 500 ℃ for 30 hrs and 700 ℃ for 100 hrs, respectively.

By contrast, porous Fe_2O_3 layer with almost no presence of other metal elements was formed in the case of an uncoated steel sample after oxidation. This implied that the Fe_2O_3 layer was formed via the outward Fe diffusion. XRD results confirmed the formation of Fe_2O_3 layer on the surface of the uncoated specimens after oxidation (Fig. 8).

Previous work have shown that the presence of Al in the top layer of a steel can effectively improve the high temperature oxidation property of the steel [18,19]. In this study, the aluminizing process followed by the oxidation treatment generated an Al_2O_3 layer on the top, which had a high Al content. It is thus fairly reasonable to expect that aluminized steel would have a better oxidation resistance than the bare steel.

To examine the effect of the presence of Fe_2Al_5 layer on he oxidation resistance, both the aluminized and the bare AISI 4130 steels were subjected to static oxidation in the temperature range 500-700 ℃. The changes in weight (mg/cm^2) of both the steels on oxidation are plotted against the square root of the oxidation time ($t^{1/2}$) (Fig. 11). Similarly as before, the diffusion controlled growth kinetics may be written as $m=k\ t^{0.5}$, where m=specimen weight, k=kinetic parameter and t=time. The oxidation rate constants obtained are listed in Table 3. The oxidation rate constants for the coated 4130 steels are much lower than those for the uncoated steels at each tested condition. As shown in Fig. 11, the coated specimens showed a very little weight change at 700 ℃ for the

Table 3. Parabolic oxidation rate constant Kp for oxidation of t coated and uncoated systems in air

Temperature	Coated specimen Kp value	Uncoated specimen Kp value
500 °C	0.0025	0.0602
600 °C	0.0029	0.1513
700 °C	0.0036	0.1947

oxidation time up to 100 hours (0.03178 mg/cm^2). On the other hand, under similar conditions, the uncoated specimen showed a much larger weight change of 2.3725 mg/cm^2. The reason for this large difference is possibly due to limited oxygen diffusion through the dense Al_2O_3 surface layer to come in contact with the metal underneath in the coated specimen. However, the uncoated steel suffers greater a weight change due to rapid oxidation of the steel, which can be explained by vaporization of the surface element volatilization upon oxidation. Therefore, the current research shows that aluminizing treatments have greatly improved the oxidation resistance of AISI 4130 steel.

4. SUMMARY

A Fe_2Al_5 layer was synthesized on the AISI 4130 steels by the pack cementation at various temperatures, within the range of 500-700 °C. The activation energy of growth of the Fe_2Al_5 layer was 53.70 kJ mol^{-1}. During the oxidation of the Fe_2Al_5 layer in the temperature range 500~700 °C, a thin layer of alumina (Al_2O_3) was formed on the surface. An evaluation of oxidation rate constants in the temperature range of 500-700 °C showed that the coated samples were significantly lower than that of the uncoated samples by about two orders of the magnitude. The results obtained in the current study show that aluminizing process greatly improves the oxidation resistance of AISI 4130 steel.

ACKNOWLEDGEMENTS

JSP appreciates financial support of Basic Science Research Program through the National Research Foundation of Korea (NRF) funded by the Ministry of Education, Science and Technology (contract No. 2013R1A1A2007650).

REFERENCES

1. T. V. Philip, Ultrahigh-strength steels. *ASM handbook,* Volume 1, *Properties and Selection: Irons, Steels, and High Performance Alloys*, p.211, ASM International, USA (2003).
2. D. B. Lee, *Korean J. Met. Mater.* **52**, 899 (2014).
3. J. Y. Choi, S. W. Hwang, M. C. Ha, and K. T. Park, *Met. Mater. Int*. **20**, 893 (2014).
4. S. K. Kwan, Y. M. Kong, and J. H. Park, *Met. Mater. Int*. **20**, 959 (2014).
5. E. N'Dah , S. Tsipas, M. P. Hieero, and F. J. Perez, *Corros Sci* **49**, 3850 (2007).
6. B. Helene and B. V. Jean, *Procedia Eng*. **2**, 917 (2010).
7. A. Aguero, J. Garciade Blas, R. Muelas, A. Sanchez, and S. Tripas, *Mater. Sci. Forum* **369-372**, 939 (2001).
8. Z. D. Xiang, J. S. Burnell-Gray, and P. K. Datta, *J. Mater. Sci.* **36**, 5673 (2001).
9. Z. D. Xiang and P. K. Datta, *Acta Mater.*, **54**, 4453 (2006).
10. B. L. Bates, Y. Q. Wang, Y. Zhang, and B. A. Pint, *Surface & Coatings Technol* **204**, 766 (2009).
11. B. Ching-Yuan, L. Yi-Jun, and K. Chun-Hao*, Surface & Coatings Technol* **183**, 74 (2004).
12. Z. Zhan, L. Zhong, L. Jianxiong, L. Li, Z. Li, and P. Liao, *Applied Surface Science* **256**, 3874 (2010).
13. P. F. Tortorelli and K. Natesan, *Mater Sci Eng* A**258**, 115 (1998).
14. H. Okamoto, *Phase diagrams for binary alloys*, ASM International, p.31, USA (1992).
15. V. Behrani *Ph.D. Thesis*, Georgia Institute of Technology, USA (2007).
16. V. Jindal, V. C. Srivastava, A. Das, and R. N. Ghosh, *Materials Letters* **60**, 1758 (2006).
17. Z. D. Xiang and P. K. Datta, *Surface and Coatings Technology* **184**, 108 (2004).
18. J. Li, J. Wang and X. Holly, *Mater Sci Technol* **19**, 657 (2003).
19. M. A. Montealegre, J. L. Gonzalez-Carrasco, and M. A. Munoz-Morris, *Intermetallics* **9**, 487 (2001).